Interaction of the Phospholipid Head Group with Representative Quartz and Aluminosilicate Structures: An Ab initio Study

James A. Snyder*,† and Jeffry D. Madura‡

Health Effects Laboratory Division, National Institute for Occupational Safety and Health, Centers for Disease Control and Prevention, Morgantown, West Virginia 26505-2888, and Center for Computational Sciences, Department of Chemistry and Biochemistry, Duquesne University, 600 Forbes Avenue, Pittsburgh, Pennsylvania 15282

Received: October 26, 2007; Revised Manuscript Received: March 10, 2008

Silica dust particles in the form of quartz (but not kaolin) have been hypothesized to promote pulmonary diseases such as silicosis. The hypothesis is that quartz and kaolin have a comparable membranolytic potential on a specific surface area basis, and they have a comparable cytotoxic potential for lavaged pulmonary macrophages. Suppression of the cytotoxic activity occurs when these dust particles are treated with dipalmitoylphosphatidylcholine (DPPC), a common phospholipid component of the lung pulmonary surfactant. However, the enzyme phospholipase A2 is known to digest the phospholipid component more readily in the presence of quartz than kaolin. Since surface silanol (Si−OH) and aluminol (Al−OH) groups may interact differently with the phospholipid, an understanding of the selective removal of phospholipid by PLA2 may explain in vivo differences in cytotoxicity between quartz and kaolin. To develop some insight into this phenomenon, the interaction between a phospholipid and silica particles was examined by performing ab initio DFT calculations on clusters constructed with small (one or two silica tetrahedral units) representative parts of the silicate surface and the phospholipid head group. The clusters consisted of a phospholipid head group or functional groups from the head group complexed with $Si(OSiH_3)_3OH$, $Al(OSiH_3)_3OH^-$ or $Al(OSiH_3)_3OH_2$. Fully optimized geometries of the complexes were used to determine binding energies, −OH vibrational frequency shifts, and NMR chemical shieldings. Results indicate that interaction of the protonated aluminol group ($Al–OH_2^+$) with the phosphate portion of the head group is strongest, while interaction of the $–OH_2^+$ group with the trimethyl−choline moiety of the head group is weakest. The presence of the choline moiety increased the magnitude of the –OH vibrational frequency shifts, and the shifts were significantly larger in complexes with protonated aluminol groups relative to silanol complexes. Analysis of ChelpG atomic charges shows that a net transfer of charge occurs from the silica unit to the head group within the complexes.

1. Introduction

Workers with exposures to certain respirable dusts are at high risk of developing pulmonary diseases such as silicosis or coal workers pneumoconiosis. Fine respirable-sized crystalline silicon dioxide mineral dusts (quartz or other polymorphs) are well-documented etiological agents for pulmonary fibrosis by epidemiological studies of human occupational exposures and by animal model inhalation or installation studies.[1] Moreover, there is sufficient evidence that crystalline silica exposures can increase the risk of lung cancer.[2]

The precise mechanism of silica cytotoxicity at the molecular level is not completely known. Upon deposition in the lung, the respirable dust surfaces may be conditioned by interaction with biological fluids and materials such as surfactant components of the pulmonary bronchiole-alveolar surface.[3] Hence, adsorption processes on silica dusts play an important role in understanding the pathogenic origin of pneumoconiosis.

Crystalline silica exposures cause silicosis, while silica in the form of aluminum silicates (clays, kaolin) does not. A significant anomaly is that while quartz is more pathogenic in vivo for fibrosis than clay, the two dusts are comparably cytotoxic in vitro.[4]

In vitro short-term bioassays studies have shown that both quartz and kaolin dusts have a comparable membranolytic potential on a specific surface area basis, and they have a comparable cytotoxic potential for lavaged pulmonary macrophages.[4] Suppression of the cytolytic activity results from treatment of the dusts with dipalmitoylphosphatidylcholine (DPPC), a common phospholipid component of the lung pulmonary surfactant.[5–8] DPPC adsorption onto the dust particle surfaces fully eliminates the cytotoxic activities of the dusts. However, the membranolytic activity of both dusts is partly to fully restored after treatment with phospholipase A_2 (PLA2), an enzyme normally associated with cellular plasma membranes and lysozomes. PLA2 digests and removes the adsorbed DPPC from the dusts. The DPPC surfactant coating was lost more readily from quartz than from kaolin, consequently resulting in a more rapid restoration of hemolytic activity for quartz. This indicates a mineral-specific difference in the digestion of DPPC adsorbed onto minerals.[9] Other studies have indicated that the mineral specificity occurs for neutral pH phospholipase systems but not for phospholipase digestion under conditions of acidic pH phospholipase digestion.[10,11] Silica particles are presumably coated with phospholipid upon deposition in the lung surfactant

* To whom correspondence should be addressed. Telephone: (304) 285-6364. Fax: (304) 285-6126. E-mail: zyu4@cdc.gov.
† Centers for Disease Control and Prevention.
‡ Duquesne University.

10.1021/jp7103769 CCC: $40.75
Published on Web 05/14/2008

and subsequently phagocytozed by macrophages, where the conditioned particles are exposed to PLA2 enzyme, possibly in the lysosome. It is known that some PLA2 enzymes work under neutral pH and others under more acidic pH conditions. Hence, if the phospholipid coating is initially removed under more acidic pH, both kaolinite and quartz particles could induce membranolysis and become reconditioned a second time and taken up by other (deeper lying) epithelial or interstitial that expose the conditioned particles to a PLA2, which acts in near neutral conditions. At that stage, more of the protective phospholipid layer may be removed on quartz than on kaolinite, allowing quartz to induce its disruptive (membranolytic) effect leading to the observed scarring and fibrosis.

NMR experiments on the interaction of DPPC with silica particles indicate that the phosphate group of DPPC is coordinated to surface hydroxyls.[12–14] More recent NMR results suggest that the (positively charged) choline unit of DPPC is also immobile on quartz surfaces but is unrestricted toward motion on kaolinite.[15] An additional feature of aluminol groups is that they are amphoteric and may exist either in the unprotonated ($-Al-OH$) or protonated ($-Al-OH_2^+$) state.

In a previous theoretical study,[16] the interaction of $Si(OH)_4$ with the dimethyl phosphate (DMP) anion was investigated, and an interaction energy of 14 kcal/mol per hydrogen bond was reported for a complex having C_1 symmetry. A more recent theoretical study examined the interaction of dimethyl methylphosphonate with amorphous SiO_2.[17] The present study is concerned with the individual influence of the other moieties of the phospholipid, namely, the positively charged choline unit $-CH_2CH_2N(CH_3)_3^+$, on the interaction with silanol and aluminol groups. PLA2 enzymes are considerably more active toward aggregates (micelles or cell membranes) of phospholipids than toward individual monomers. In the case of secretory PLA2 enzymes, this is primarily due to so-called interfacial catalysis, in which specific surface residues on the enzyme collectively interact with a set of phospholipid head groups in the aggregate. This allows efficient positioning of a hydrophobic channel in the enzyme, over a targeted phospholipid, which is configurationally poised for entry into the hydrophobic channel as a result of its interactions within the aggregate assemble.[18–20] Strict requirements on the orientation of the *sn*-1 and *sn*-2 substituents of the glycerol backbone are evidently necessary for entry of the substrate into the active site region of the enzyme. The phospholipid is expected to adsorb onto the silica particles as a bilayer, in which the outer layer is facing the solvent, while the inner layer consists of phospholipid head groups (with water) orientated toward the silica surface. This would leave the outer layer available for digestive hydrolysis by the enzyme, involving such interfacial catalysis. The experimental studies show that about 30% of the adsorbed phospholipid is initially rapidly removed from both quartz and kaolinite, followed by a slower rate of removal for quartz and much slower yet for kaolinite (at pH 7).[10,11] Interfacial catalysis and facilitated diffusion of the phospholipids constituting the inner layer, in which the head groups face the silica surface, would presumably also necessitate the positioning of the enzyme over the head groups, although the presence of the silica particle would be expected to modify the efficiency of the process Alternatively, it is possible that the observed differences in the rate of phospholipid digestion from quartz and kaolin by the enzyme are determined by the strengths of the interaction of part of the head group, such as the phosphate group, with surface silanols and aluminols. This can influence the desorption of phospholipid monomers away from the aggregate layer and the availability of the phospholipid monomer to the enzyme. However, it may still be possible that the energetics of the catalyzed ester hydrolysis reaction itself is influenced by interactions with surface hydroxyls after the substrate is positioned within the active site of the enzyme, perhaps resulting from a random encounter by the enzyme–substrate complex with an exposed silica surface. Although the nature of the glycerol backbone *sn*-3 substituent appears not to influence enzyme activity, the influence of surface hydroxyl groups interacting with this substituent is not known. Several crystal structures exits for the PLA2 enzyme with a transition-state phospholipid analogue in the active site, for which a space-filling model shows some of the *sn*-3 substituent exposed at the surface of the enzyme. A future goal will be to use combined quantum mechanical/molecular mechanics (QM/MM) methods to examine whether surface silanol and aluminol groups can influence the energetics of the PLA2 enzyme catalysis. Therefore, the data presented in this study may also be useful for interpretation of results from more detailed future computational studies. The primary goal of this study, however, was to identify significant differences in the interaction between protonated aluminol and silanol groups with the phospholipid head group.

2. Methods

The use of an optional $-SiH_3$ rather than –OH as a terminating group provides the additional control with respect to restriction to either single silanol ($\equiv Si-OH$) or double silanol [geminal silanol: $>Si-(OH)_2$] groups within the cluster. The presence of two hydroxyl groups allows the possibility to form two hydrogen bonds with the phosphate group. Unlike a complex of $Si(OH)_4$ with dimethyl phosphate (DMP) having C_1 symmetry, which can form two identical hydrogen bonds, for the clusters used in this work, two hydrogen bonds with the phosphate group would each be expected to be slightly different, except perhaps for the hydrogen bonds with DMP. Therefore, a comparison can be made of the contribution of each individual hydrogen bond to the binding energy of the cluster. The clusters were extended in order to examine the influence of a nearby (vicinal) silanol or aluminol group from a neighboring tetrahedral unit on the interaction between the primary silanol or aluminol group and the phosphate unit of the head group. This was done using the structures $HO-Si(OR)_2-O-Si(OR)_2-OH$ (SIL−SIL) and $HO-Si(OR)_2-O-Al(OR)_2-OH_2$ (SIL−ALU). In this study, Al was tetrahedrally coordinated to four nearest-neighbor oxygens, which is an approximation to the octahedral coordination known to exist for Al in aluminosilicates. This approximation and these kinds of structures were successfully used in earlier investigations involving silica surface interactions and properties.[21–26] Binding energies (B.E.), selected vibrational frequency shifts, and ^{31}P NMR chemical shieldings were calculated and compared for the different structures.

Full geometry optimizations were performed for each cluster, first at the restricted Hartree–Fock level using the 3-21+G(d,p) basis set followed by a density functional theory calculation using the B3LYP level of theory with the 6-31+G(d,p) basis set. These geometries were then used to calculate NMR chemical shieldings using the gauge-independent atomic orbital (GIAO) method at the B3LYP level with the 6-311+G(3df,2p) basis set. The DFT-optimized geometries were used to calculate vibrational frequencies, which were scaled by a factor of 0.9613.[27] All monomers and complexes were confirmed to be minima. Binding energies were computed by subtracting the sum of the total energies of the two monomers in a cluster, each optimized at the same level of theory and basis set, from

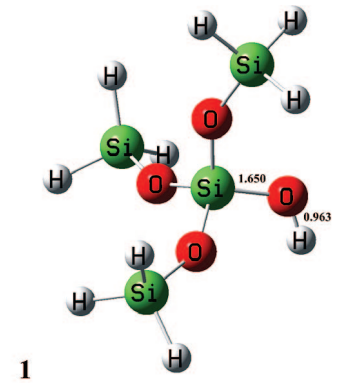

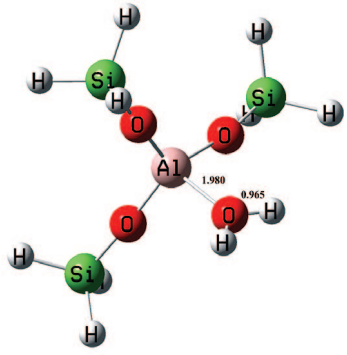

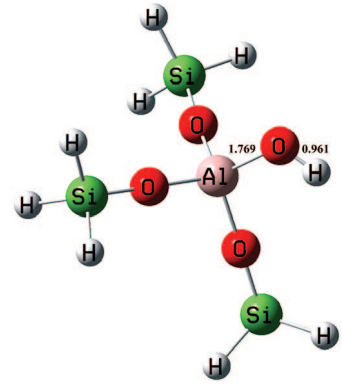

Figure 1. Optimized structures of the isolated quartz (SIL) and aluminosilicate (ALU, ALU^-) monomers used in the complexes with the phospholipid head group.

the total energy of the cluster complex. The zero-point energy-corrected binding enthalpies were similarly computed and corrected to 298 K. Estimates of the basis set superposition error (BSSE) for the binding energies were calculated using the counterpoise method.[28] The Gaussian 98 program[29] was used for all calculations.

3. Results and Discussion

3.1. Geometries and Binding Energies. Optimized geometries for the isolated structures of $Si(OR)_3OH$, (SIL) $Al(OR)_3OH^-$, (ALU^-), and $Al(OR)_3OH_2$ (ALU) are given in Figure 1. Figure 2 presents the optimized geometries for clusters of SIL complexed with smaller segments of the full head group. The cluster containing only a representative choline unit [$-CH_2CH_2N(CH_3)_3^+$] of the head group is labeled as SIL−Ch (complex **4**). A cluster containing only the phosphate unit of the head group, represented as dimethyl phosphate (DMP) interacting with SIL, is labeled as SIL−DMP (complex **5**). Complex **6** contains a segment of the head group consisting of only the choline unit and the phosphate unit and is labeled as SIL−Ch−Ph. In Figure 3, the analogous optimized structures are presented for complexes of ALU^- and the same phospholipid fragments (complexes **7**–**9**). Binding energies and zero-point-corrected enthalpies for each of the complexes are given in Table 1. In this study, the addition of the glycerol/hydrocarbon tail was found not to contribute more than 2–3 kcal/mol of additional change in the B.E. and only minor structural changes relative to the complexes including only the choline or the choline and phosphate unit. Results including the effect of the glycerol/hydrocarbon tail backbone are therefore excluded.

The optimized geometry for the unprotonated aluminol complex of ALU^- with the whole head group, denoted ALU^-−head (complex **10**) is shown in Figure 4. Table 1 indicates that the B.E. for the ALU−Ch−Ph cluster (**9**) is −37.0 kcal/mol, while the B.E. for complex ALU^-−head (**10**) is −23.0 kcal/mol. Hence, the interaction between the phosphate unit of the phospholipid and the protonated aluminol group is more favorable relative to interaction with the unprotonated aluminol group. Comparison of ALU−Ch−Ph (**9**) and ALU^-−head (**10**) also shows that the interaction of the protonated aluminol group with the phosphate group involves a proton transfer to the oxygen of the P−O bond directly involved in the hydrogen-bonded interaction with the aluminol group. Moreover, the hydrogen bond is more linear (176.3° in **9** compared with 147.3° in **10**) and, hence, stronger for the complex with the protonated aluminol. In an ab initio study of the interaction of acetic acid/acetate with protonated and unprotonated aluminol groups,[26] the B.E. for interaction with the protonated aluminol group was found to be favored relative to interaction with an unprotonated form by approximately −25 kcal/mol.

Figures 3 and 4 also show the distance between the nitrogen atom of the choline unit and the donor oxygen atom of the hydrogen-bonded aluminol group. This N−O distance is longer (4.405 Å) for the complex with the protonated aluminol, ALU−Ch−Ph (**9**), compared to the value for the complex with the unprotonated aluminol ALU^-−head (3.513 Å) (**10**).

From Table 1, it can be seen that the interaction with the isolated representative choline analogue, $CH_3CH_2N(CH_3)_3^+$, is weakest for both SIL−Ch and ALU−Ch complexes (**4** and **9**), both B.E.'s being approximately −10 kcal/mol. Moreover, the H_2O molecule in the optimized structure for complex **9** is oriented opposite to the positively charged choline analogue.

To analyze the effect on the interaction between the silanol or aluminol group and the phosphate unit of the phospholipid due to the presence of the functional groups, in particular, the choline moiety, comparisons can be made relative to SIL−DMP and ALU−DMP (**5** and **10**). From Table 1, the B.E. of complex **5** is −26.0 kcal/mol. However, the B.E. for SIL−Ch−Ph (**6**) (−18.5 kcal/mol) is smaller in magnitude than that of SIL−DMP (**5**) by 7.5 kcal/mol, indicating that the presence of the positively charged choline moiety significantly weakens the interaction between the phosphate unit and the silanol group. Comparison of the B.E.'s in Table 1 for ALU−DMP and ALU−Ch−Ph (**8** and **9**) shows that an analogous trend also applies to the effect of the choline moiety on the interaction between the protonated aluminol group and the phosphate unit of the head group. The effect of the choline unit on interaction with aluminol groups is slightly more pronounced, as can be seen by comparing the binding energies for complexes **8** and **9** for which the difference is 8.2 kcal/mol. Although solvent effects are not included in this kind of study, it is significant to note that the strength of

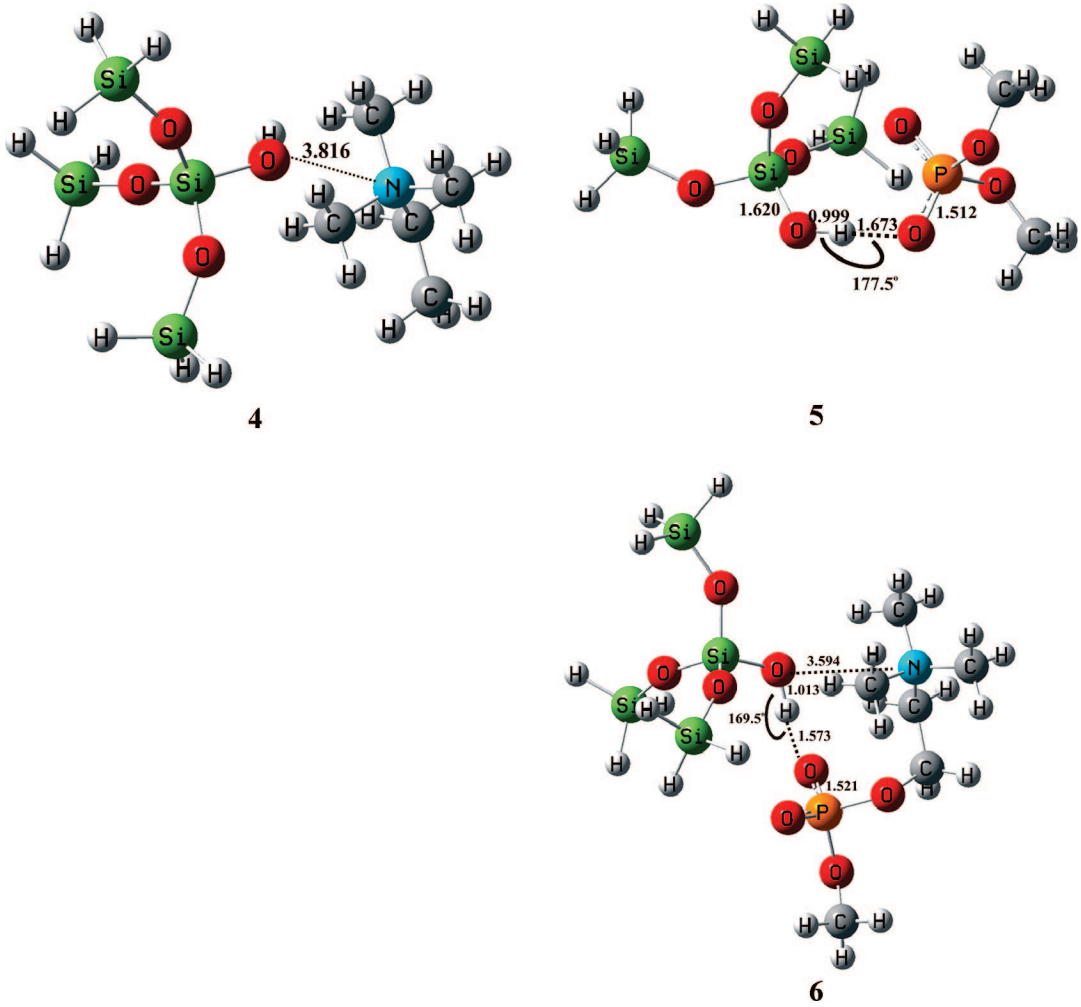

Figure 2. Optimized structures of complexes of a representative quartz fragment with the choline moiety (SIL−Ch), the phosphate group (SIL−Ph), and the phosphate group + choline unit (SIL−Ch−Ph).

the hydrogen-bonded interaction with silica surface hydroxyl groups appears to be stronger in the absence of the choline moiety, in general. The phospholipid monomer in complexes such as SIL−DMP (**5**) can be considered as an analogue of an anionic phospholipid. Normal pulmonary surfactant contains some anionic phospholipids in addition to zwitterionic phospholipids such as DPPC. The ratio of zwitterionic to anionic phospholipids is approximately 7:3.[30] If, indeed, it was found that anionic phospholipids compete with zwitterionic phospholipids, with respect to interaction with a quartz surface, it would be interesting to determine if adsorption of anionic phospholipids onto quartz has a similar effect on the digestive action of the PLA2, as seen with in the experimental comparisons of kaolinite with quartz when both are initially treated with DPPC. However, conclusions based on the results given here must be interpreted with caution since they represent interactions in a vacuum and ignore contributions such as solvent and counterions.

The B.E. associated with interaction with the unprotonated aluminol group in ALU$^-$−head (**10**), −23.0 kcal/mol, is larger in magnitude than that for SIL−Ch−Ph (**6**), −18.5 kcal/mol. It is difficult to compare a difference of 4–5 kcal/mol since the calculations were performed using only small silica structures and the magnitude of the consequent uncertainties introduced into the results are ambiguous. The BSSE-corrected binding energies in Table 1 are all smaller than the uncorrected values by 2−3 kcal/mol. Hence, for all aforementioned comparisons above involving uncorrected B.E. values, the same relative pattern of differences appears for comparisons using the BSSE-corrected values. This hydrogen-bonded interaction becomes even stronger (as discussed above) for the complex with a protonated aluminol group, ALU−Ch−Ph (**9**), for which the B.E. becomes −37.0 kcal/mol. Moreover, Table 1 shows that the magnitude of the binding energies and, hence, the strength of the interactions with the phosphate unit are greater for the complexes with the protonated aluminol group, ALU−DMP and ALU−Ch−Ph, (**8** and **9**), compared with that for the complexes involving interaction with a silanol group, SIL−DMP and SIL−Ch−Ph (**5** and **6**). As Figure 3 shows, in each of the aluminol−head group complexes ALU−DMP and ALU−Ch−Ph (**8** and **9**), there is a proton transfer from the protonated aluminol group to the phosphate group. Ab initio studies have shown that the hydrogen-bonded interaction of a protonated aluminol group with the acetate anion is stronger compared with interaction with a silanol group.[26] It is also possible to view complexes **8** and **9** as involving a hydrogen bond between the unprotonated aluminol group (Al−OH) and the protonated phosphate of the phospholipid monomer. However, since the pK_a of typical phosphates is on the order of 2, it is more likely that the phosphate moiety in biological systems acts as a hydrogen-bond acceptor rather than as a donor.[16]

Figure 3 shows the distance between the nitrogen atom of the choline unit and the donor oxygen atom of the hydrogen-bonded aluminol group. The analogous atom pair distances are shorter in each of the silanol complexes shown in Figure 2.

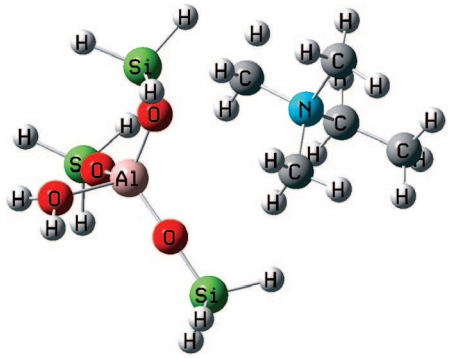

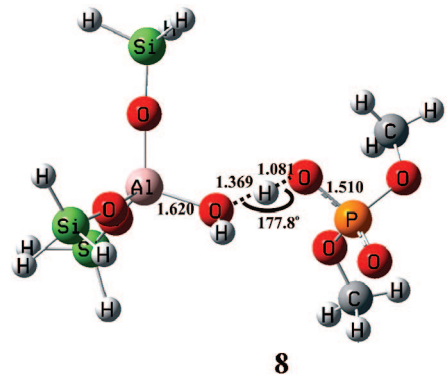

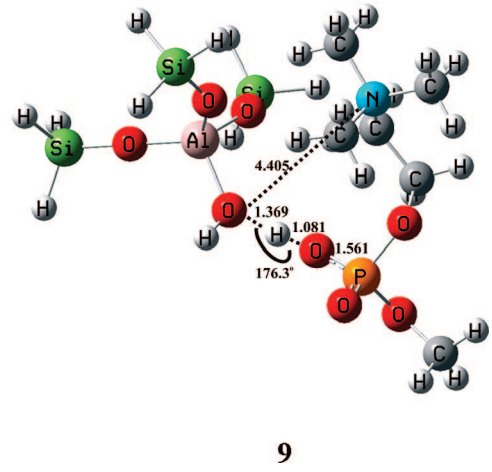

Figure 3. Optimized structures of complexes of a representative protonated aluminosilicate fragment with the choline moiety (ALU−Ch), the phosphate group (ALU−Ph), and the phosphate group + choline unit (ALU−Ch−Ph).

TABLE 1: Binding Energies (B.E.; kcal/mol), Thermal Enthalpy Change (Δ*H*; kcal/mol) for Binding (Including Zero-Point Energy Correction), Si(Al)−O−H Frequency Shifts (Δ*ν*; cm^{-1}), and IR Intensity Ratios (in Parenthesis) Relative to Isolated Silica Monomers for Complexes [4]–[15][a]

complex	B.E.	Δ*H*	Δ*ν*
4 SIL−Ch	−10.5(−9.27)	−9.1 [b]	
5 SIL−DMP	−26.0(−23.6)	−24.6	−712(17.6)
6 SIL−Ch−Ph	−18.5(−15.9)	−17.2	−976(21.0)
7 ALU−Ch	−10.8(−9.83)	−8.5 [b]	
8 ALU−DMP	−45.2(−43.8)	−45.4	−1903(62.2)
9 ALU−Ch−Ph	−37.0(−33.8)	−36.0	−1857(62.2)
10 ALU$^-$−head	−23.0(−20.3)	−20.8	−127(24.9)
11 SIL(OH)$_2$−head	−25.6(−22.5)	−24.0	−629(30.7); −715(5.7)
12 ALU(OH)$_2^-$−head	−24.0(−21.6)	−22.4	−94(30.5)
13 ALU(OH)OH$_2$−head	−37.5(−34.1)	−37.1	−248(5.6) [−OH]; −1796(48.5) [−OH$_2$]
14 SIL−SIL−Ch−Ph	−19.6(−16.8)	−18.3	−997(22.7)
15 SIL−ALU−Ch−Ph	−31.9(−28.4)	−30.8	−1496(41.8)

[a] Ch and Ph denote choline and phosphate units, respectively. B.E. values corrected for BSSE are given in parenthesis. [b] Negligible.

This result and the differences noted above for the binding energies may corroborate recent experimental NMR findings, which indicate that for silica particles treated with DPPC, the choline unit of DPPC is immobile on quartz surfaces but remains relatively unrestricted toward motion on aluminosilicate.[15]

Figures 2 and 3 illustrate how the choline moiety influences the geometry of the hydrogen bond between the silanol or aluminol group and the acceptor oxygen atom of the phosphate unit relative to SIL−DMP (**5**) and ALU−DMP (**8**), respectively. Comparison of the geometries in SIL−DMP (**5**) and SIL−Ch−Ph (**6**) shows that the hydrogen-bond angle decreases from 177.5

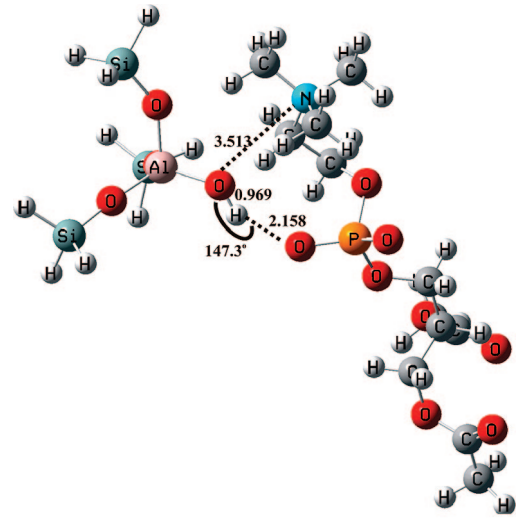

Figure 4. Optimized structures of the unprotonated aluminol complex of Al(OR)$_3$OH$^-$ with the whole head group (ALU$^-$−head).

in **5** to 169.5° in **6**. However, inspection of the hydrogen-bond geometries of ALU−DMP and ALU−Ch−Ph (**8** and **9**) indicates that the presence of the choline moiety, which is more distant from the hydrogen bond than that in the silanol complexes, has only a negligible effect on the hydrogen-bond geometry in ALU−Ch−Ph (**9**).

3.2. Estimated Atomic Charges. Table 2 lists the ChelpG[31] charges for select atoms within the complexes and the net sum of the charges on the isolated monomers and the monomers

TABLE 2: ChelpG Charges for Atoms Si(Al)−O−H of the Isolated Monomers 1–3 and for Atoms Si(Al)−O···H···O_p−P−O_p' of Complexes 4–10 and the Total Charge on the Silica and Head Group Monomers of Each Cluster or Isolated Structure

complex (monomer)	Si (Al)	O	H	O_p	O_p'	P	silica monomer	head group monomer
1 SIL	1.377	−0.767	0.409				0	
2 ALU	1.277	−0.698	0.432				0	
3 ALU^-	1.280	−0.943	0.370				−1	
5 SIL−DMP	1.299	−0.860	0.502	−0.760	−0.644	1.235	−0.223	−0.777
6 SIL−Ch-Ph	1.341	−0.874	0.525	−0.830	−0.703	1.314	−0.042	0.042
8 ALU−DMP	1.166	−0.885	0.509	−0.674	−0.714	1.203	−0.353	−0.647
9 ALU−Ch−Ph	1.244	−0.971	0.541	−0.740	−0.685	1.262	−0.238	0.238
10 ALU^-−head	1.184	−0.973	0.454	−0.786	−0.759	1.295	−0.915	−0.085
Isolated head group of complex **5** and **8** (DMP)				−0.813	−0.813	1.328		−1
Isolated head group of complex **6** and **9** (−Ch−Ph)				−0.803	−0.750	1.316		0

TABLE 3: Comparison of Mulliken, Natural Atomic Orbital (NAO), and Atomic Polarization Tensor (APT) Charges on the Atoms Si(Al)−O···H···O_p−P−O_p' of the SIL−DMP (5) and ALU−DMP (8) Complexes

complex	Si (Al)	O	H	O_p	O_p'	P
5 SIL−DMP						
ChelpG	1.299	−0.860	0.502	−0.760	−0.644	1.235
Mulliken	2.353	−1.047	0.471	−0.920	−1.057	2.134
NBO	2.575	−1.180	0.557	−1.165	−1.188	2.593
APT	2.638	−1.111	0.611	−1.064	−1.061	2.372
8 ALU−DMP						
ChelpG	1.166	−0.885	0.509	−0.674	−0.714	1.203
Mulliken	−0.703	−0.599	0.567	−0.936	−0.803	2.023
NBO	2.194	−1.188	0.564	−1.105	−1.117	2.605
APT	2.379	−1.137	0.904	−1.245	−0.917	2.461

within the complexes. For comparison, the Mulliken charges,[32] natural atomic orbital (NAO),[33–40] and atomic polarization tensor (APT)[41] charges on select atoms of the SIL−DMP (**5**) and ALU−DMP (**8**) complexes are given in Table 3. Table 3 illustrates that three methods of assigning charge place unrealistic charges (greater than 2e in magnitude) on the P and Si(−OH) atoms. This motivated the use of ChelpG charges for the following analysis.

Table 2 shows that more electron density appears on the Al atom and a concomitant more positive charge is imparted onto the hydrogen-bond donor oxygen of the aluminol group, relative to structures with a silanol group. For example, for SIL−DMP (complex **5**), the charges on the Si−O−H atoms are 2.353, −1.047, and 0.471e, compared with charges of −0.703, −0.599, and 0.567e on the Al−O−H atoms of ALU−DMP (**8**). Except for ALU^-−head (**10**), there is a net transfer of electron density from the head groups onto the silica monomer. This is in agreement with earlier calculations with, for example, $Si(OH)_4$ and DMP.[16] More electron density is transferred in the protonated aluminol clusters relative to silanol complexes. Again, the presence of the choline unit influences the transfer of electron density. The choline unit decreases the net amount of electron density shifted from the head group to the silica monomer in each cluster. However, the choline unit causes more electron density to appear on the hydroxyl oxygen and slightly less on the central metal [compare the Si and O atoms in SIL−DMP (**5**) and in SIL−Ch−Ph (**6**) in Table 2, for example].

Table 2 also includes the ChelpG charges on the O_P' atom (not coordinated in the hydrogen bond). The electron density on this atom varies slightly for aluminol complexes and silanol complexes and is influenced by the presence or absence of the choline moiety.

The mechanism of action of the PLA2 enzyme has been studied computationally using QM/MM methods.[42–44] A schematic depiction of the active site of the enzyme is reproduced in Figure 5. The mechanism involves a Ca^{2+} ion coordinated with the carbonyl oxygen of the ester linkage and O_P' atom of the phospholipids. It is possible that variation of the charge on the O_P' atom, or change of the total charge of the head group of the magnitude shown in Table 2, due to the presence of silanol or aluminol groups coordinated with the head group could influence the energetics/action of the PLA2 enzyme.

3.3. Vibrational Analysis. DFT calculations on hydrogen-bonded interactions between silanol groups and phosphates have estimated that the vibrational frequency associated with the silanol O−H stretching mode decreases by as much as 600 cm^{-1}, although these values are evidently considered to be overestimates due to limitations in the ability of DFT methods to fully describe the O−H bond.[16,21–26] However, Bermudez[17] reports a theoretical DFT Si−O−H frequency shift of approximately 420 cm^{-1} for the interaction the P═O oxygen of dimethyl methylphosphonate with surface silanols on a cluster representing an amorphous SiO_2 surface. This is compared with the reported experimental value of 524 cm^{-1}, which indicates an underestimate. Similarly, the Si−O−H frequency shift reported for a periodic DFT calculation of NH_3 adsorbed on the edingtonite silica surface is underestimated by approximately 300 cm^{-1}.[45] Therefore, we anticipate that our reported vibrational frequencies underestimate the experimentally observed values by 100−300 cm^{-1}.

The calculated vibrational red shifts associated with the silanol and aluminol (O−H) stretching mode relative to the isolated silica monomers for complexes SIL−DMP (**5**), SIL−Ch−Ph (**6**), ALU−DMP (**8**), and ALU−Ch−Ph (**9**) are listed in Table 1. The frequency shift is on the order of 700 cm^{-1} for the silanol in SIL−DMP (**5**) but increases to 976 cm^{-1} for the silanol in SIL−Ch−Ph (**6**), for which the choline moiety is present. A similar trend occurs for the protonated aluminosilicate clusters, but the magnitudes of the shifts are substantially larger, increasing to 1857 cm^{-1} for ALU−Ch−Ph (**9**), and the ratios of IR intensities are larger. As noted above, interaction of protonated aluminol groups with the phospholipid head group

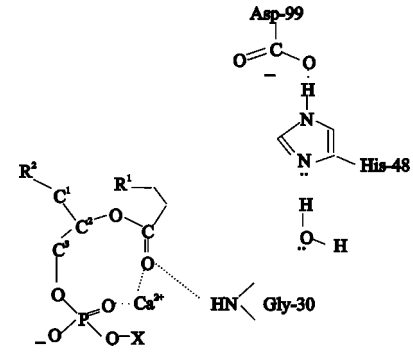

Figure 5. Active site model of the PLA2 enzyme; taken from ref 43.

TABLE 4: Isotropic ^{31}P NMR Chemical Shieldings (σ; ppm) for Select Complexes and for Isolated Monomers of the Head Group Used in the Complexes

complex	σ (^{31}P)
5 SIL−DMP	280
6 SIL−Ch−Ph	282
8 ALU−DMP	285
9 ALU−Ch−Ph	285
isolated head group monomer of [**5**] and [**8**] (DMP)	281
isolated head group monomer of [**6**] and ([**9**] (−Ch−Ph)	282

involves a proton transfer to the O_P atom of the phosphate unit of the head group. The O−H vibration then corresponds more to a O−H group of a protonated phosphate than an aluminol group. However, comparison of SIL−DMP and SIL−Ch−Ph (**5** and **6**) with ALU−DMP and ALU−Ch−Ph (**8** and **9**) shows that the O−H distance involving the donor oxygen of the hydrogen bond (O_P atom in the case of aluminol complexes) is longer in the protonated aluminol complexes. Comparing SIL−DMP and ALU−DMP (**5** and **8**), for example, these distances are 0.999 and 1.081 Å, respectively. Hence, although there is proton transfer, the resulting O−H distance is longer in the aluminol complex relative to that in the silanol complex, and this may contribute to a weaker bond, which perhaps accounts, in some part, for the larger vibrational red shifts calculated for complexes ALU−DMP and ALU−Ch−Ph (**8** and **9**).

3.4. NMR Chemical Shieldings. ^{31}P NMR chemical shieldings (σ) were calculated for complexes **5**, **6**, **8**, and **9** and for the optimized geometry of the isolated phospholipid head group monomer of each of those clusters. These values are given in Table 4. For the isolated head group structures, relative to the head group fragment of SIL−DMP (**5**) and ALU−DMP (**8**), the σ(^{31}P) value increases from 280 ppm for DMP to 282 ppm for −Ch−Ph by the addition of the choline moiety of the monomer from SIL−Ch−Ph (**6**) and ALU−Ch−Ph (**9**). The influence of the two kinds of silica monomers is also evident from Table 4. The chemical shieldings are larger by as much as 3 ppm in the aluminol clusters relative to that in the silanol clusters. Reference to Tables 2 and 4 shows that increased ^{31}P chemical shieldings of each aluminol complex, ALU−DMP (**8**) and ALU−Ch-Ph (**9**), can be correlated with a larger share of electron density (smaller positive charges) on the P atom in a given aluminol complex relative to that on the analogous silanol complexes, SIL−DMP (**5**) and SIL−Ch−Ph (**6**). This is true despite the fact that more electron density is transferred from the head group to the aluminol monomers compared with that transferred to the silanol monomers.

3.5. Effect of Geminal Silanol Groups. Besides single silanol groups, cleaved silica surfaces are also characterized by the presence of geminol silanol groups, in which two hydroxyls are bound to a single Si atom. The optimized geometries for complexes with two hydroxyl groups on a Si or Al atom, SIL(OH)$_2$−head (**11**), ALU(OH)$_2^-$−head (**12**), and ALU(OH)-OH$_2$−head (**13**) are shown in Figure 6. Table 1 shows that the addition of the second hydrogen bond increases the binding energy in the silanol complex SIL(OH)$_2$−head (**11**), as expected, but only by an additional −7.6 kcal/mol relative to the −18.0 kcal/mol for SIL−Ch−Ph (**6**). Evidently, the presence of a second hydrogen bond with a second unprotonated aluminol group ALU(OH)$_2^-$−head (**12**) is not favored, and the minimum-energy structure with two such hydrogen bonds could not be found. It should be noted that the donor H to acceptor O atom distances for the hydrogen bond between an unprotonated aluminol group and the phosphate oxygens are longer and

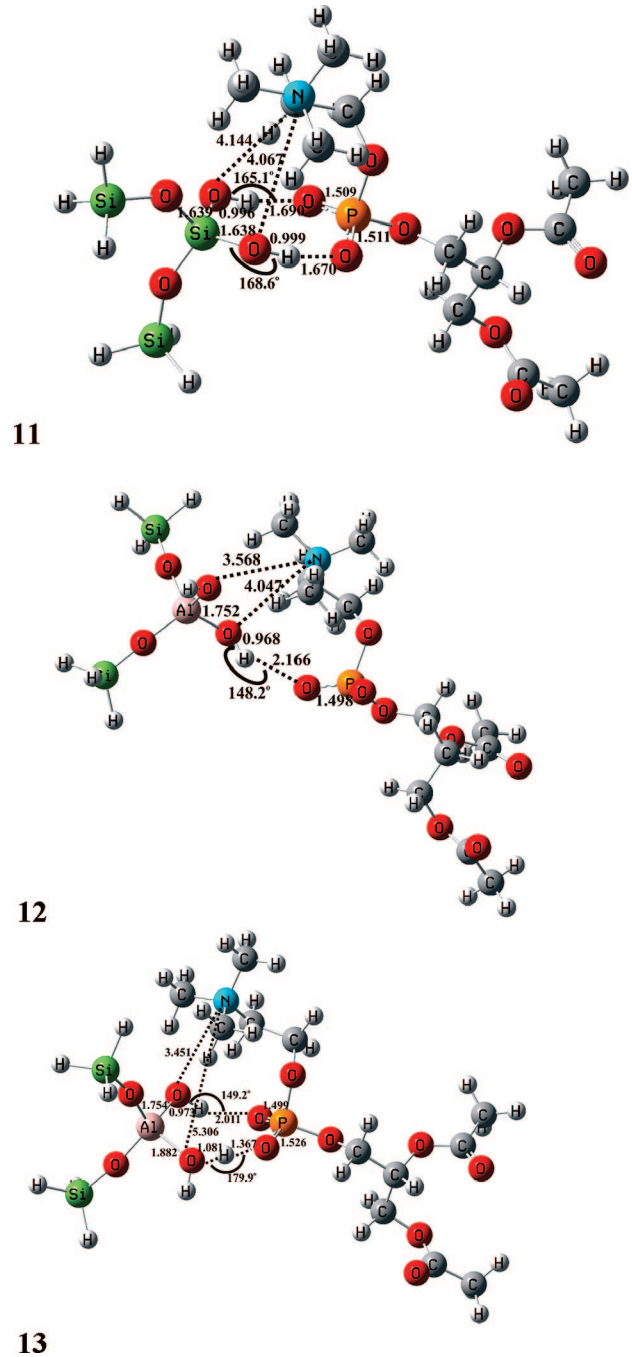

Figure 6. The optimized geometries resulting from two possible hydrogen-bonded interactions between the phosphate unit of the head group and two hydroxyl groups on the Si atom [SIL(OH)$_2$−head] or Al atom [ALU(OH)$_2^-$−head].

contribute to weaker hydrogen bonding relative to that for hydrogen bonds involving silanol groups [compare 1.572 Å for SIL−Ch−Ph (**6**) with 2.158 Å for ALU$^-$−head (**10**) and 1.699 Å in SIL(OH)$_2$−head, (**11**) with 2.166 Å for ALU(OH)$_2^-$−head, (**12**)]. Protonation of one of the two aluminol groups, ALU(OH)OH$_2$−head (**13**) increases the binding energy to −37.5 kcal/mol, and two hydrogen bonds are now formed with the phosphate head group. Again, the second hydrogen bond does not make any additional contribution to the binding energy relative to the for the interaction between a single protonated aluminol group and the phosphate (B.E for ALU−Ch−Ph (**9**) is −37.0 kcal/mol). The distance from the hydrogen-bonded protonated aluminol group to the choline is, again, longer in

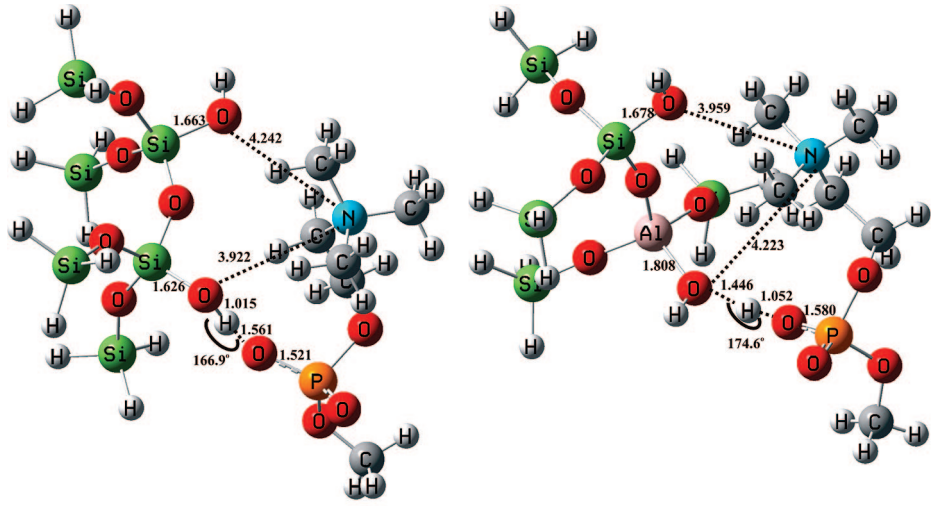

14 15

Figure 7. Optimized structure of a complex of the head group with a two-silica representative quartz and aluminosilicate unit (SIL−SIL−Ch−Ph and SIL−ALU−Ch−Ph).

that for ALU(OH)OH_2 (**13**) (Figure 6) compared with the analogous distance for unprotonated aluminol in ALU$(OH)_2^-$ (**12**) or the hydrogen-bonded silanol in SIL$(OH)_2$ (**11**).

3.6. Effect of a Neighboring Tetrahedral Silica Unit. The next level of approximation beyond the simple clusters considered so far is to include a second silica monomer unit, which presents a second surface hydroxyl group. Neighboring silanols such as this are generally called vicinal silanols. For kaolinite, depending on how the surface might be cleaved, it is possible to have either another Si atom or another Al atom in the second silica position. Figure 7 presents optimized geometries for the two-silica unit of the representative quartz−head group complex SIL−SIL−Ch−Ph (**14**) and one example of a larger cluster for a representative aluminosilicate−head group SIL−ALU−Ch−Ph (**15**). The isolated monomer geometries are provided in Figure 8. Table 1 indicates that the binding energies are not influenced appreciably by the presence of a neighboring silanol group relative to those of a single isolated silanol group. The distance between the hydrogen-bonded hydroxyl and the choline unit is still larger in the protonated aluminol SIL−ALU−Ch−Ph (**15**), but the difference compared with this distance in SIL−SIL−Ch−Ph (**14**) is not as pronounced. Comparison of the B.E.'s for complexes ALU−Ch−Ph (**9**) and SIL−ALU−Ch−Ph (**15**) indicates that the presence of a neighboring silanol group can affect the binding energy by at least 5 kcal/mol. In an ab initio study of the adsorption of the chemical warfare compound dimethyl methylphosphonate on γ-Al_2O_3 clusters of varying size, the largest difference in (BSSE-corrected) binding affinities was also found to be on this order.[46] Although effects such as cluster size may be investigated in future studies, it is not expected to alter the primary result of this study, which was the finding that protonated aluminols can increases the magnitude of the binding energy relative to silanol groups by at least 10 kcal/mol (16 kcal/mol in this study).

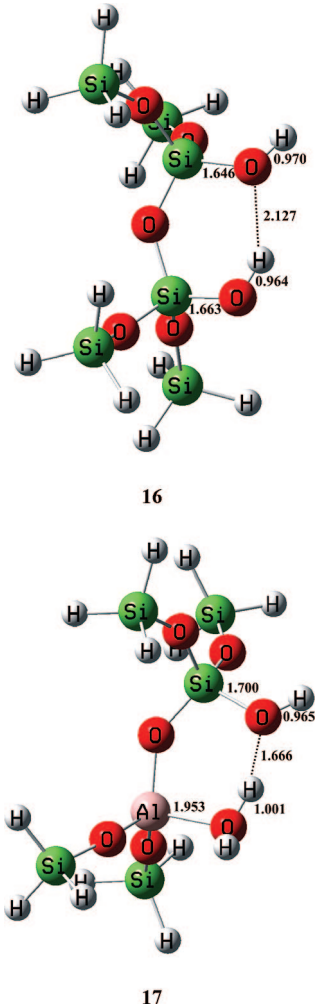

16

17

Figure 8. Optimized structures of the isolated silica monomer units of complexes **14** and **15** in Figure 7.

Conclusion

In this study, the interaction of phospholipid and fragments of phospholipid with clusters representing quartz and aluminosilicate surfaces was examined using DFT calculations. BSSE-corrected binding energies are all within 5 kcal/mol of the uncorrected values and predict the same trend in relative interaction energies for all of the studied complexes. The interaction of an unprotonated aluminol group (Al−OH) with the phospholipid head group is stronger compared to that with a silanol group (Si−OH), the binding energy being approximately 5–6 kcal/mol larger in magnitude. Interaction of a protonated aluminol group ($-OH_2^+$) with the head group

increases the magnitude of the binding energy by as much as 16 kcal/mol relative to the interaction of a silanol group. The presence of the choline moiety in the head group has a significant influence on the magnitude of the interaction with silica surface hydroxyl groups. The positively charged choline group can reduce the magnitude of the binding energy of the complex by as much as 7 kcal/mol. The choline moiety is more distant from the protonated aluminol group compared with the unprotonated aluminol or silanol group. It was found that ChelpG charges were required to produce realistic charges (values less than 2e in magnitude) on Si, Al, and P atoms in the complexes, when compared with Mulliken, NBO, and APT charges. Interaction of the phosphate unit of the head group with silanol and aluminol groups causes a net change in the total charge of the head group, which coordinates with active site residues (e.g., a Ca^{2+} ion) in the PLA2 enzyme. This may influence the action of the phospholipase A2 (PLA2) enzyme. Future studies will employ QM/MM methods to investigate the influence of aluminol (protonated and unprotonated) and silanol groups on the energetics of the active site mechanism of the PLA2 enzyme. The presence of the choline unit in the complexes was found to increase the Si(Al)−OH vibrational frequency shifts slightly. In complexes with the protonated aluminol group, there is a proton transfer to the anionic (P−O) oxygen, which results in a large increase in the frequency shift. Calculated ^{31}P NMR chemical shieldings were increased slightly by the presence of the choline unit and were also larger in aluminol complexes relative to those in silanol complexes. These results may be useful for eventually understanding experimental differences observed for the rate of removal of the zwitterionic phospholipid DPPC from silica versus aluminosilicate surfaces by the action the PLA2 enzyme.

Acknowledgment. The authors wish to thank the National Cancer Institute's Advanced Biomedical Computing Center (NCI-ABCC) for the use of their computational facilities. The authors thank W. E. Wallace for insightful discussion. The findings and conclusions in this report are those of the authors and do not necessarily represent the views of the National Institute for Occupational Safety and Health.

References and Notes

(1) In *Silica and Silica-Induced Lung Diseases*; Castranova, V., Vallyathan, V., Wallace, W. A., Eds.; CRC Press: Boca Raton, FL, 1996.

(2) *Silica, Some Silicates, Coal Dust and Para-Aramid Fibrils*; International Agency for Research on Cancer (IARC) Monographs on the Evaluation of the Carcinogenic Risk of Chemical to Humans; World Health Organization: Lyon, France.; 1997.

(3) Wright, J. R.; Clements, J. A. *Am. Rev. Respir. Dis.* **1987**, *136*, 426.

(4) Vallyathan, V.; Schwegler, D.; Reasor, M.; Stettler, L.; Green, F. H. Y. *Ann. Occup. Hyg.* **1988**, *32* (Suppl. 1), 279.

(5) Emerson, R. J.; Davis, G. S. *Environ. Health Perspect.* **1983**, *51*, 81.

(6) Schimmelpfeng, J.; Seidel, A. *J. Toxicol. Environ. Health* **1999**, *33*, 131.

(7) Schimmelpfeng, J.; Drosselmeyer, E.; Hofheinz, V.; Seidel, A. *Environ. Health Perspect.* **1992**, *97*, 225.

(8) Wallace, W. E.; Vallyathan, V.; Keane, M. J.; Robinson, V. *J. Toxicol. Environ. Health* **1985**, *16*, 415.

(9) Wallace, W. E.; Keane, M. J.; Hill, C. A.; Vallyathan, V.; Regad, E. D. *J. Toxicol. Environ. Health* **1992**, *37*, 391.

(10) Hill, C. A.; Wallace, W. E.; Keane, M. J.; Mike, P. S. *Cell Biol. Toxicol.* **1995**, *11*, 119.

(11) Liu, X.; Keane, M. J.; Harrison, J. C.; Cilento, E. V.; Ong, T.; Wallace, W. E. *Toxicol. Lett.* **1998**, *96*, 77.

(12) Deppasse, J.; Warlus, J. *J. Colloid Sci.* **1976**, *56*, 618.

(13) Allison, A. *Sci. Am.* **1967**, *217*, 62.

(14) Chunbo, Y.; Daqing, L.; Aizhou, N.; Jiazuan, J. *J. Colloid Interface Sci.* **1995**, *172*, 536.

(15) Murray, D. K.; Harrison, J. C.; Wallace, W. E. *J. Colloid Interface Sci.* **2005**, *288*, 166.

(16) Murashov, V. V.; Leszczynski, J. *J. Phys. Chem. A* **1999**, *103*, 1228.

(17) Bermudez, V. M. *J. Phys. Chem. C* **2008**, *111*, 9314.

(18) Linderoth, L.; Andresen, T. L.; Jorgensen, K.; Madsen, R.; Peters, G. *Biophys. J.* **2008**, *94*, 14.

(19) Berg, O. G.; Gelb, M. H.; Tsai, M.; Jain, M. K. *Chem. Rev.* **2001**, *101*, 2613.

(20) Scott, D. L.; Sigler, P. B. *Adv. Protein Chem.* **1994**, *45*, 53.

(21) Konecny, R. *J. Phys. Chem. B* **2001**, *105*, 6221.

(22) Gibbs, G. V.; Downs, J. W.; Boisen, M. B., Jr. In *Reviews Mineralogy*; Heaney, P. J., Prewitt, C. T., Gibbs, G. V., Eds.; MSA: Washington, DC, 1994; Vol. 29, p 331.

(23) Casanovas, J.; Illas, F.; Pacchioni, G. *Chem. Phys. Lett.* **2000**, *326*, 523.

(24) Ferrari, A. M.; Ugliengo, P.; Garrone, E. *J. Phys. Chem.* **1993**, *97*, 2671.

(25) Sauer, J.; Ugliengo, P.; Garrone, E.; Saunders, V. R. *Chem. Rev.* **1994**, *94*, 2095.

(26) Aquino, A. J. A.; Tunega, D.; Haberhauer, G.; Gerzabek, M. H.; Lischka, H. *J. Comput. Chem.* **2003**, *24*, 1853.

(27) Wong, M. W.; Wiberg, K. B.; Frisch, M. J. *J. Chem. Phys.* **1991**, *95*, 8991.

(28) Boys, S. F.; Bernardi, F. *Mol. Phys.* **1970**, *19*, 553.

(29) Frisch, M. J.; Trucks, G. W.; Schlegel, H. B.; Scusera, G. E.; Robb, M. A.; Cheeseman, J. R.; Zakrzewski, V. G.; Montgomery, J. A.; Stratmann, Jr., R. E.; Burant, J. C.; Dapprich, S.; Millam, J. M.; Daniels, A. D.; Kudin, K. N.; Strain, M. C.; Farkas, O.; Tomasi, J.; Barone, V.; Cossi, M.; Cammi, R.; Mennucci, B.; Pomelli, C.; Adamo, C.; Clifford, S.; Ochterski, J.; Petersson, G. A.; Ayala, P. Y.; Cui, Q.; Morokuma, K.; Malick, D. K.; Rabuck, A. D.; Raghavachari, K.; Foresman, J. B.; Cioslowski, J.; Ortiz, J. V.; Baboul, A. G.; Stefanov, B. B.; Liu, G.; Liashenko, A.; Piskorz, P.; Komaromi, I.; Gomperts, R.; Martin, R. L.; Fox, D. J.; Keith, T.; Al-Laham, M. A.; Peng, C. Y.; Nanayakkara, A.; Gonzalez, C.; Challacombe, M.; Gill, P. M. W.; Johnson, B.; Chen, W.; Wong, M. W.; Andres, J. L.; Gonzalez, C.; Head-Gordon, M.; Replogle, E. S.; Pople, J. A. *Gaussian 98*, revision A.7; Gaussian, Inc.: Pittsburgh, PA, 1998.

(30) Kaznessis, Y. N.; Kim, S.; Larson, R. G. *Biophys. J.* **2002**, *82*, 1731.

(31) Breneman, C. M.; Wiberg, K. B. *J. Comput. Chem.* **1990**, *11*, 361.

(32) Mulliken, R. S. *J. Chem. Phys.* **1955**, *23*, 1833.

(33) Carpenter, J. E.; Weinhold, F. *J. Mol. Struct.: Theochem* **1988**, *169*, 41.

(34) Carpenter, J. E. Ph.D. Thesis, University of Wisconsin, Madison, WI, 1987.

(35) Foster, J. P.; Weinhold, F. *J. Am. Chem. Soc.* **1980**, *102*, 7211.

(36) Reed, A. E.; Weinhold, F. *J. Chem. Phys.* **1983**, *78*, 4066.

(37) Reed, A. E.; Weinhold, F. *J. Chem. Phys.* **1983**, 1736.

(38) Reed, A. E.; Weinstock, R. B.; Weinhold, F. *J. Chem. Phys.* **1985**, *83*, 735.

(39) Reed, A. E.; Curtiss, L. A.; Weinhold, F. *Chem. Rev.* **1988**, *88*, 899.

(40) Weinhold, F.; Carpenter, J. E. *Plenum* **1988**, 227.

(41) Cioslowski, J. *J. Am. Chem. Soc.* **1989**, *111*, 8333.

(42) Waszkowycz, B.; Hillier, I. H.; Gensmantel, N.; Payling, D. W. *J. Chem. Soc., Perkin Trans. 2* **1989**, 1795.

(43) Waszkowycz, B.; Hillier, I. H.; Gensmantel, N.; Payling, D. W. *J. Chem. Soc., Perkin Trans. 2* **1991**, 225.

(44) Waszkowycz, B.; Hillier, I. H.; Gensmantel, N.; Payling, D. W. *J. Chem. Soc., Perkin Trans. 2* **1991**, 1819.

(45) Civalleri, B.; Garrone, E.; Ugliengo, P. *J. Phys. Chem. B* **1998**, *102*, 2373.

(46) Bermudez, V. M. *Phys. Chem. C* **2008**, *111*, 3719.

JP7103769